Contact Lens and Anterior Eye 42 (2019) 55–62

Contents lists available at ScienceDirect

Contact Lens and Anterior Eye

journal homepage: www.elsevier.com/locate/clae

Scleral contact lens thickness profiles: The relationship between average and centre lens thickness

Stephen J. Vincent*, David Alonso-Caneiro, Henry Kricancic, Michael J. Collins

Contact Lens and Visual Optics Laboratory, School of Optometry and Vision Science, Queensland University of Technology, Australia

ARTICLE INFO

Keywords:
Scleral contact lens
Scleral lens thickness
OCT imaging
Oxygen transmissibility

ABSTRACT

Purpose: To develop a methodology to reliably determine the thickness profile of scleral contact lenses and examine the relationship between the centre and average lens thickness for a range of lens designs and back vertex powers.

Methods: High-resolution images of 37 scleral trial lenses (Epicon LC, Rose K2 XL and ICD 16.5) were captured using an optical coherence tomographer, and their thickness profiles were generated after correcting for known measurement artefacts. Centre lens thickness values were compared with manual lens gauge measurements, and repeatability was assessed by comparing average thickness values derived from orthogonal meridians of each lens.

Results: The imaging technique displayed a high level of agreement with a manual lens gauge for centre thickness measurements; mean difference 5 ± 9 μm (95% LoA −14 to +23 μm), and a very high level of repeatability; mean difference between orthogonal meridians 1 ± 3 μm (95% LoA −6 to +8 μm). Lens thickness profiles varied between lens designs, with distance from the lens centre, and with back vertex power. Increasing back vertex powers resulted in a significant over or underestimation (up to 33% for high minus powers) of the average lens thickness based on the centre lens thickness.

Conclusions: The thickness of scleral contact lenses varies with distance from the lens centre and the back vertex power. The average lens thickness value derived from the entire lens provides a more appropriate representation of the true lens thickness and should be used in the calculation of scleral lens oxygen transmissibility.

1. Introduction

The thickness profile of a rigid contact lens is influenced by a range of factors including the back vertex power, the front and back optic zone radii, the optic zone and total lens diameters, the transition zones between peripheral curves and the refractive index of the material (for soft contact lenses, the water content or hydration state of the material also influences lens thickness) [1,2]. These factors also determine the thickness profile of modern scleral contact lenses, however, scleral lenses are much thicker (with centre thickness values typically between 300 and 400 μm for smaller diameter miniscleral lenses, but up to 1300 μm for larger diameters) [3] than rigid corneal lenses (~150 μm) in order to minimise lens flexure during wear and handling. This increased centre lens thickness directly impacts upon oxygen delivery to the cornea, despite the use of highly oxygen permeable materials [4].

While several clinical studies have confirmed that minimal corneal oedema occurs with daily wear of modern high Dk sealed scleral lenses in young healthy eyes (typically 2% or less) [5,6], irrespective of the magnitude of apical clearance [7,8], older eyes may display a greater hypoxic response [9]. Pullum et al. [4] observed a linear decrease in corneal oedema during daily wear of large diameter high Dk scleral lenses (Dk 115) as centre lens thickness was systematically reduced from 1200 to 300 μm, however, a plateau in the reduction of corneal oedema was observed between 300 and 150 μm. This suggests that for high Dk scleral lenses, minimising the centre thickness to ~300 μm may be of benefit to reduce anterior segment hypoxia, particularly in eyes with a reduced endothelial cell count. However, this may not be feasible if a high plus power is required, or if significant lens flexure occurs (which often requires an increase in the centre or junctional thickness).

The lens centre thickness differs from the average lens thickness to varying degrees. Previous modelling [1,2] and measurement [10,11] of various soft contact lenses indicate substantial thickness variations with increasing back vertex powers; consequently, isolated local measurements of central lens thickness significantly underestimate the average lens thickness (derived from the entire lens or several local regions

* Corresponding author at: Contact Lens and Visual Optics Laboratory, School of Optometry and Vision Science, Queensland University of Technology, Room D513, O Block, Victoria Park Road, Kelvin Grove 4059, Brisbane, Queensland, Australia.
E-mail address: sj.vincent@qut.edu.au (S.J. Vincent).

https://doi.org/10.1016/j.clae.2018.03.002
Received 9 January 2018; Received in revised form 22 February 2018; Accepted 6 March 2018

across a lens) for negatively powered lenses, and overestimate the average lens thickness for positively powered lenses which has implications for accurately estimating the theoretical oxygen transmissibility. While scleral lenses will exhibit a similar relationship between the centre and average lens thickness, despite a greater overall thickness and total diameter compared to other types of contact lenses, currently no studies have examined the thickness profile of scleral contact lenses in detail.

The relationship between the centre thickness of scleral contact lenses and the average thickness derived from measurements across the entire lens, rather than a single centre thickness value, provides important information regarding the true oxygen transmissibility of scleral contact lenses. In this study, we describe a technique to measure the thickness profile of scleral contact lenses using an optical coherence tomographer (OCT), including image corrections to minimise the influence of known measurement artefacts (e.g. optical distortion and instrument assumed refractive indices) [12–14] and present cross-sectional lens thickness data for a range of scleral lenses (one corneo-scleral and two miniscleral designs).

2. Methods

2.1. Contact lenses

Thirty-seven rotationally symmetric RGP trial lenses from three different diagnostic fitting sets were imaged in this study. The EpiCon LC (Capricornia Contact Lens, Queensland, Australia) is a corneo-scleral contact lens; seven EpiCon LC trial lenses with median peripheral curves were imaged (back optic zone radii: 6.4 to 7.6 mm, total diameter: 13.5 mm, back vertex power: −7.35 D, hexafocon A material). The Rose K2 XL (Menicon, Nagoya, Japan) is a miniscleral contact lens [15]; sixteen Rose K2 XL trial lenses with a standard edge lift were imaged (back optic zone radii: 6.0 to 8.0 mm, total diameter: 14.6 mm, back vertex power: +1.00 to −17.00 D, tisilfocon A material). The ICD 16.5 (Capricornia Contact Lens, Queensland, Australia) is a miniscleral contact lens [16]; fourteen ICD 16.5 trial lenses were imaged (back optic zone radii: 6.0 to 8.7 mm, total diameter: 16.5 mm, back vertex power: +0.75 to −15.87 D, hexafocon A material).

2.2. OCT imaging

Each contact lens was mounted securely in front of a Spectralis OCT with anterior segment module (Spectralis, Heidelberg Engineering, Heidelberg, Germany) using a custom-designed lens holder (Fig. 1) to ensure consistent and stable lens positioning during imaging. An individual lens holder was used for each lens design (total diameters of 13.5, 14.6 and 16.5 mm) which were designed using 3D CAD design software (SolidWorks) and printed using a 3D printer (Projet 3510 SD, 3D Systems) (accuracy ± 0.025 to 0.05 mm). The lens holders ensured the centre of each contact lens was aligned with the OCT measurement beam, without the unwanted application of pressure to minimise flexure during imaging. High-resolution cross sectional images (the average of 100 images per B-scan) were obtained along the horizontal and vertical meridians through the lens centre. The Spectralis OCT uses a super luminescent diode with a central wavelength of 870 nm, which provides images with an axial resolution of 3.9 µm and transverse resolution of 14 µm, with a scanning speed of 40,000 A-scans per second. While the comparatively shorter wavelength of the Spectralis OCT allows high-resolution imaging, this results in a reduced imaging depth (1800 µm) which does not allow an entire scleral lens (with sagittal depths of up to 5600 µm in this study) to be imaged in a single acquisition. Therefore, for each lens examined, 2–3 overlapping B-scans were captured at varying depths to ensure the entire lens was imaged.

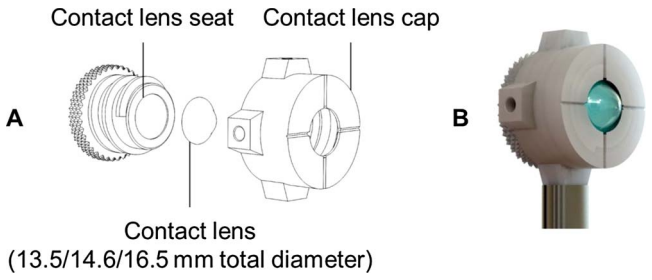

Fig. 1. An expanded view of the custom designed contact lens holder used in this study (A) and the complete assembly (B) with a miniscleral contact lens in place. For each lens design (i.e. 13.5 mm, 14.6 mm or 16.5 mm total diameter) the diameter of the contact lens seat was 0.4 mm greater than the total lens diameter with a depth of 0.5 mm.

2.3. Image processing

Since image contrast was reduced in some of the B-scans which resulted in poor visibility of the anterior and posterior contact lens boundaries, additional contrast-enhanced methods were applied for intensity compensation [17]. The level of contrast enhancement was controlled by adjusting the algorithm's intensity exponent parameter (n) and two different copies were output for each B-scan with an intensity exponent of n = 1 or n = 2. Images of the entire horizontal and vertical cross-sections were constructed for each lens using Adobe Photoshop (Adobe Systems Incorporated, San Jose, USA). For all cross-sectional images, the original B-scan (i.e. without contrast enhancement) for each imaging depth was imported into the workspace. If the contact lens boundaries displayed reduced visibility, an enhanced-contrast B-scan was imported instead. Overlapping regions were then manually aligned and 'stitched' together as a single image (Fig. 2A). Customised software was developed to manually mark the contact lens boundaries in the final stitched image. A single observer selected a number of points along the anterior and posterior contact lens boundaries (between 19 and 25 points for each boundary), and a cubic spline interpolation was used to fit the points and extract the boundary of interest (Fig. 2B).

2.4. Image correction and thickness calculation

All OCT images are affected by optical distortion such that the true curvature and thickness of a contact lens cannot be derived directly from an OCT image due to the curvature and refractive index of the material imaged (i.e. the position and contour of the back surface of the contact lens in an OCT image is influenced by the refractive effect of the front surface). In addition, the Spectralis OCT assumes a uniform tissue refractive index of 1.40 to calculate thickness measures. Therefore, additional procedures were carried out on the segmented data from each OCT image; firstly to correct the boundary locations for the effects of refraction at the interface boundary (using an approach based on Snell's law [18]) assuming a refractive index of 1.437 for the tisilfocon A material and 1.415 for the hexafocon A material. This approach has been used previously to correct for refractive distortion when imaging through ocular tissues [19]. These refractive distortion corrected boundary locations were then used to extract the thickness data along the horizontal and vertical meridian of each contact lens. Due to the curvature of a contact lens, a standard axial thickness calculation (along the A-scan) cannot be used, because the lens curvature will bias the thickness measurement. For this study, the Laplace method was used to calculate the thickness data between the anterior and posterior contact lens boundaries [20]. The Laplace method calculates thicknesses along lines that connect two boundaries which are orthogonal to each boundary, do not intersect with other lines, and are nominally parallel [21]. Using this approach, the lens thickness is defined as the length of the line of flow between the two surfaces assigned different potentials, which could be considered the likely passage of oxygen through the lens. Since each lens imaged was a rotationally symmetric design, the individual thickness profiles presented are the average data from four

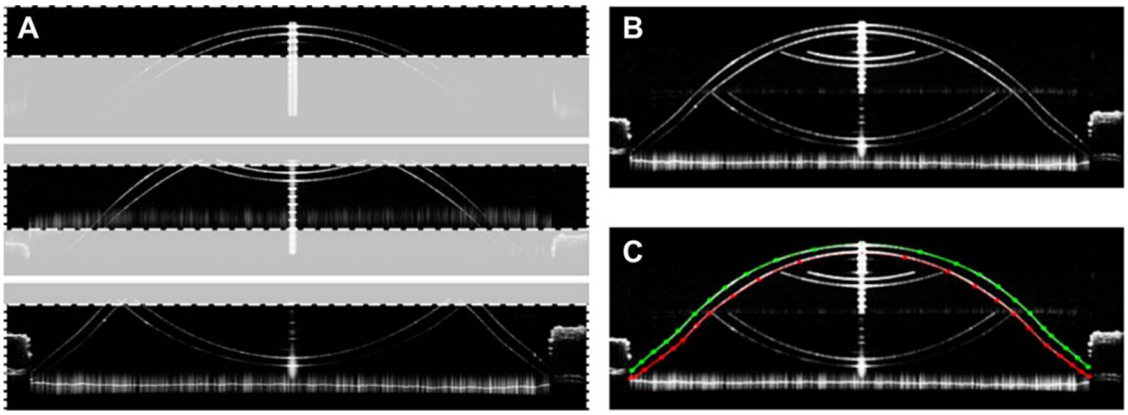

Fig. 2. A representative set of multiple B-scans taken at varying depths required to image an entire contact lens (A). The highlighted regions of the scans were extracted for stitching. The stitched image (B) and the same stitched image overlaid with user selected data points for boundary segmentation and the fitted spline curves (C) (in this example there were 23 points for the anterior [green] and posterior [red] contact lens boundaries).

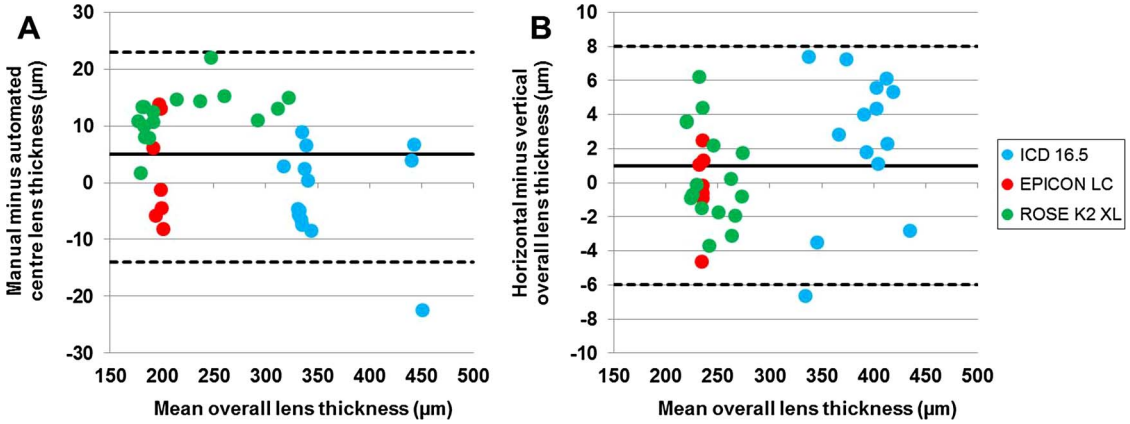

Fig. 3. (A) Bland-Altman plot of the agreement between the manual lens gauge and the OCT method for measures of lens centre thickness. (B) Bland-Altman plot of the repeatability of measures of average lens thickness derived using the OCT method (comparing measurements obtained along the horizontal and vertical meridian from the same rotationally symmetric lens). Solid black lines represent the mean difference and dashed black lines represent the upper and lower 95% limits of agreement. Data obtained from each lens design is highlighted in each panel (ICD 16.5–blue, Epicon LC – red, Rose-K2 XL – green), however the mean difference and limits of agreement are calculated from all lens designs considered together. (For interpretation of the references to colour in this figure legend, the reader is referred to the web version of this article.)

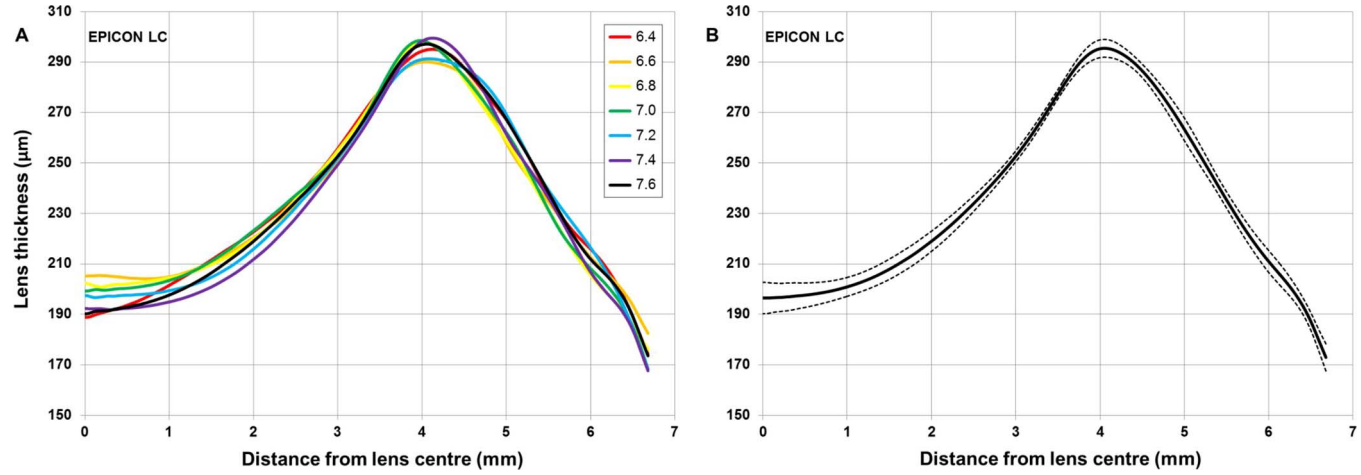

Fig. 4. Individual lens thickness profiles across a half-diameter (from lens centre to edge) for the EpiCon LC lens (median peripheral curve, back vertex power −7.35 D) for a range of back optic zone radii (A) and the mean thickness profile (B) of the seven individual lenses plotted in (A). The solid black line in (B) represents the mean and the dashed black lines represent one standard deviation of the mean.

half-diameters (i.e. two measurements from the lens centre to lens edge in both the horizontal and vertical meridians). The midpoint of the imaged lens diameter was used as the lens centre for each meridian. The absolute difference (mean ± standard deviation) between the imaged lens diameter and the manufacturer specified lens diameter was 0.13 ± 0.13 mm averaged across both meridians of the 37 scleral lenses (note the total lens diameter manufacturing tolerance for scleral lenses is ± 0.25 mm [22]). The centre thickness, minimum and

Table 1
Descriptive lens thickness data for the EpiCon LC including the nominal and measured lens centre thickness (minimum, maximum and average values derived from data across the entire lens, 13.5 mm total diameter).

LENS	THICKNESS (μm)				
BOZR (mm)/BVP (D)	NOMINAL	CENTRE	MINIMUM	MAXIMUM	AVERAGE
6.4/−7.35	170	189	167	295	236
6.6/−7.35	170	205	170	290	236
6.8/−7.35	170	202	166	298	235
7.0/−7.35	170	199	167	299	236
7.2/−7.35	170	197	165	291	235
7.4/−7.35	170	192	164	299	232
7.6/−7.35	170	190	174	297	235

BOZR – back optic zone radius, BVP – back vertex power.

maximum thickness, and average lens thickness were calculated for each lens along with the difference between the centre thickness and average lens thickness.

2.5. Agreement analysis (centre lens thickness)

The centre lens thickness of each trial lens was measured three times by an observer masked to the lens design (base curve, refractive power, and published manufacturer nominal thickness value) using a manual contact lens thickness gauge (Nippon Contact Lens Research Institute, Japan). This device provides accurate measures of central lens thickness to 10 μm; however, estimates can be made subjectively to the nearest micron. Central lens thickness measurements obtained using both the manual contact lens gauge (an average of three measurements) and the OCT imaging method (to the nearest micron), were compared using an intraclass correlation and Bland-Altman analysis [23].

2.6. Repeatability analysis (average lens thickness)

Similar to the central thickness agreement analysis, to provide an estimate of the repeatability of the OCT imaging method, the average thickness values derived from the horizontal and vertical meridian for each trial lens (since all were rotationally symmetric designs) were compared using an intraclass correlation and Bland-Altman analysis.

3. Results

3.1. Agreement: comparison of OCT imaging and manual lens gauge (centre lens thickness)

A high level of agreement was observed between the centre lens thickness measured with the manual lens gauge and the OCT imaging method (ICC 0.994, 95% CI: 0.988–0.997). The mean relative difference between the two methods (manual gauge minus OCT) was 5 ± 9 μm (95% LoA −14 to +23 μm) (Fig. 3A), and the mean absolute difference was 9 ± 5 μm (95% LoA −1 to +20 μm).

3.2. Repeatability: comparison of OCT imaging along orthogonal meridians (average lens thickness)

A very high level of repeatability was observed for measures of average lens thickness derived along two orthogonal meridians using the OCT imaging method (ICC 0.999; 95% CI: 0.998–1.000). The mean relative difference between the two repeated measures (horizontal minus vertical) was 1 ± 3 μm (95% LoA −6 to +8 μm) (Fig. 3B), and the mean absolute difference was 3 ± 2 μm (95% LoA −1 to +7 μm).

3.3. Scleral lens thickness profiles

Scleral lens thickness profiles, presented across a half-diameter, are displayed in Figs. 4-6 for each lens design and the descriptive data (minimum, maximum, centre and average thickness) are summarised for each lens in Tables 1–3 along with the manufacturers nominal centre thickness. The profiles for each lens within a diagnostic kit are plotted individually (but are grouped together according to specific thickness profiles based on back vertex power) and as a mean (for each specific thickness profile). As expected, contact lens thickness varied considerably from the centre to the lens edge and the thickness profile varied with back vertex power.

3.3.1. EpiCon LC

Fig. 4 displays the individual (A) and mean (B) thickness profiles for

Table 2
Descriptive lens thickness data for the Rose K2 XL including the nominal and measured lens centre thickness (minimum, maximum and average values derived from data across the entire lens, 14.6 mm total diameter).

LENS	THICKNESS (μm)				
BOZR (mm)/BVP (D)	NOMINAL	CENTRE	MINIMUM	MAXIMUM	AVERAGE
6.0/−17.00	180	179	159	360	267
6.2/−14.00	180	184	180	344	263
6.4/−11.50	180	172	150	301	235
6.5/−10.25	180	178	152	295	232
6.6/−9.50	180	175	155	285	226
6.7/−8.5	180	176	166	277	225
6.8/−7.75	200	186	164	279	230
6.9/−6.75	200	179	164	261	220
7.0/−5.75	200	187	165	256	220
7.1/−4.75	200	207	166	262	236
7.2/−3.50	240	230	173	271	242
7.3/−2.75	240	237	175	268	247
7.4/−1.75	240	253	167	276	251
7.6/−0.75	280	287	168	287	264
7.8/0.00	280	305	173	305	274
8.0/+1.00	280	315	155	315	274

BOZR – back optic zone radius, BVP – back vertex power.

Table 3
Descriptive lens thickness data for the ICD 16.5 including the nominal and measured lens centre thickness (minimum, maximum and average values derived from data across the entire lens, 16.5 mm total diameter).

LENS	THICKNESS (μm)				
BOZR (mm)/SAG (μm)/BVP (D)	NOMINAL	CENTRE	MINIMUM	MAXIMUM	AVERAGE
6.03/5600/−15.87	300	337	213	570	436
6.03/5300/−12.75	300	336	195	567	419
6.14/5100/−10.75	300	331	201	575	413
6.37/4900/−8.75	300	341	195	542	402
6.49/4800/−8.00	300	349	218	536	401
6.75/4700/−6.87	300	338	216	502	388
6.03/4600/−5.87	300	334	190	431	364
6.89/4500/−4.87	300	335	173	463	371
6.13/4400/−4.12	300	339	199	415	346
6.49/4300/−3.00	300	316	205	409	334
6.89/4200/−1.87	300	334	181	418	335
7.18/4100/−1.00	420	462	230	463	407
8.04/4000/+0.25	420	439	268	439	400
8.65/3900/+0.75	420	439	211	439	389

BOZR – back optic zone radius, SAG – sagittal depth over a 15 mm chord, BVP – back vertex power.

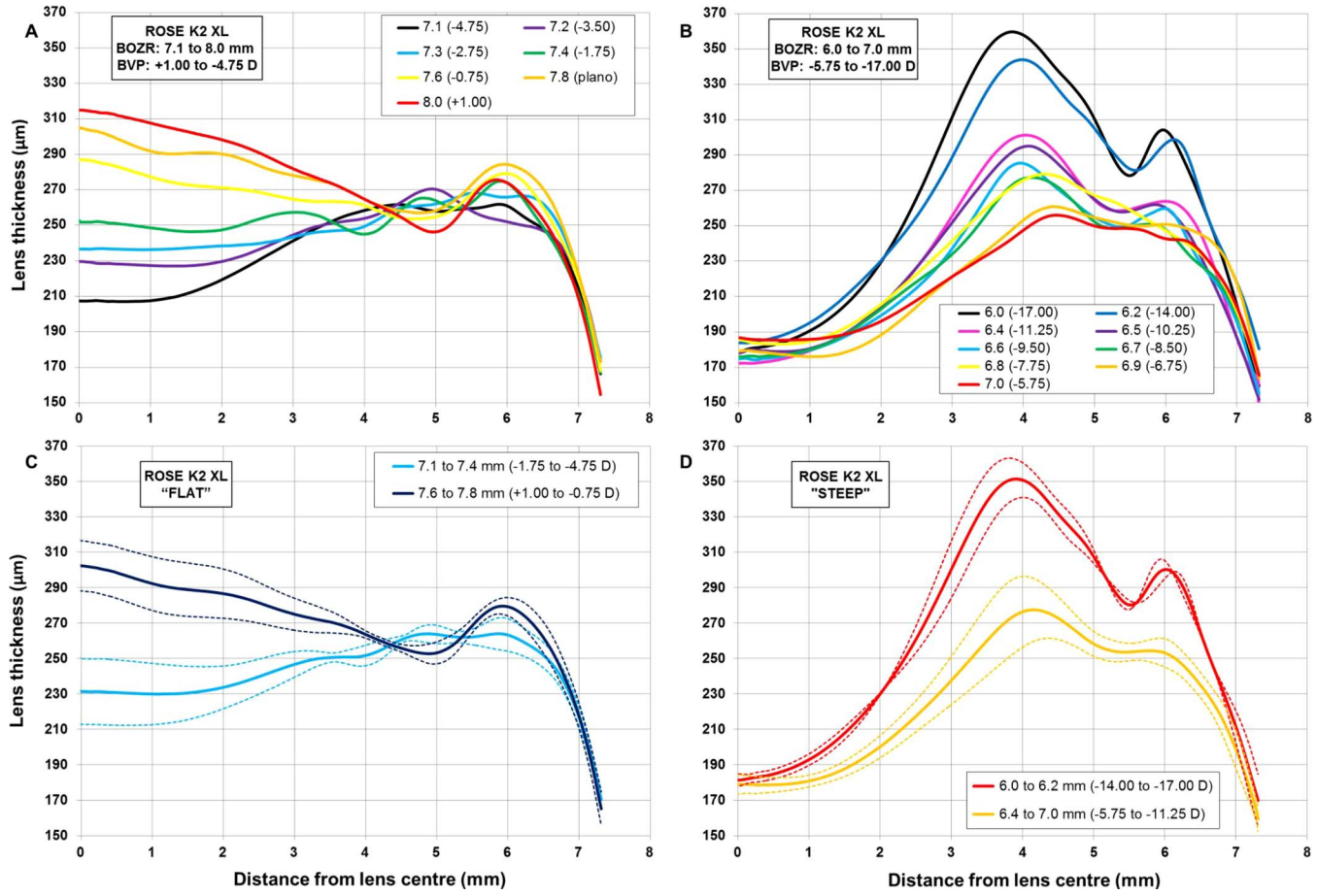

Fig. 5. Individual lens thickness profiles across a half-diameter (from lens centre to edge) for the Rose K2 XL lens design for a range of trial lenses with flatter back optic zone radii (7.1 to 8.0 mm) (A) and steeper back optic zone radii (6.0 to 7.0 mm) (B). Mean lens thickness profiles for the flatter (C) and steeper (D) back optic zone radii lenses that display different thickness profiles with respect to back vertex power. The solid lines in (C) and (D) represent the mean and the dashed lines represent one standard deviation of the mean.

the seven EpiCon LC lenses of varying back optic zone radii with the same back vertex power (−7.35 D). The mean centre thickness was 196 ± 6 µm, the maximum thickness was 296 ± 4 µm approximately 4 mm from the lens centre (i.e. the junctional thickness at the edge of the optic zone) which decreased linearly to a minimum of 167 ± 3 µm at the lens edge. The average lens thickness was 235 ± 1 µm. Fig. 4 also highlights the minimal variation between the seven lenses suggesting that alterations in the back optic zone radius have limited impact on lens thickness when controlling for back vertex power.

3.3.2. Rose K2 XL

Fig. 5 displays the individual thickness profiles for "flatter" (7.1 mm/−4.75 D to 8.0 mm/+1.00 D, Fig. 5A) and "steeper" (6.0 mm/−17.00 D to 7.0 mm/−5.75 D, Fig. 5B) Rose K2 XL lenses. Four distinct thickness profiles can be visualised in Figs. 5C and 5D with changes in back optic zone radii/back vertex power. Significant increases in junctional thickness values are evident for the steeper (high minus) lenses (Fig. 5D) compared to the flatter lenses of lower back vertex powers in Fig. 5C. All lenses displayed a rapid thinning from the peak or secondary peak in lens thickness (~6 mm from the lens centre) to the lens edge (7.3 mm).

3.3.3. ICD 16.5

Fig. 6 displays the individual thickness profiles for the ICD 16.5 lenses of "low" (3900 µm/+0.75 D to 4100 µm/−1.00 D, Fig. 6A), "medium" (4200 µm/−1.87 D to 4600 µm/−5.87 D, Fig. 6B) and "high" sagittal depths (4700 µm/−6.87 D to 5600 µm/−15.87 D, Fig. 6C) (based on the observed difference in thickness profiles for each of these lens groupings). Three distinct thickness profiles can be visualised in Fig. 6D (based on the sagittal depth over 15 mm/the back vertex power), similar to the Rose K2 XL profiles in Fig. 5C and D.

3.4. Centre thickness compared to average thickness

The centre and average lens thickness for each individual lens is presented in Tables 1–3. For the EpiCon LC, the average lens thickness was 38 ± 6 µm greater than the centre lens thickness (i.e. measurements of centre thickness underestimated the average lens thickness by ~16%). The difference between the centre and average lens thickness varied with back vertex power (Fig. 7) and followed a similar trend for the ICD 16.5 and the Rose K2 XL designs with the centre lens thickness overestimating the average lens thickness for low powers (± 1 D) by ~10%, but underestimating the average lens thickness by between ~5-33% (from −2.75 to −17 D). The variation (error) in the difference between the centre and average lens thickness with back vertex power approximates a second order polynomial function; ICD 16.5: $y = 0.13 \times^2 + 4x + 10$ ($R^2 = 0.94$) and ROSE K2 XL: $y = 0.15 \times^2 + 5x + 10$ ($R^2 = 0.99$), where y denotes the percentage error (over or under estimation) and x denotes the back vertex power (D).

4. Discussion

This study describes a novel method to image scleral contact lenses of moderate sagittal depth using an anterior segment OCT with appropriate corrections for image-related distortions to derive the

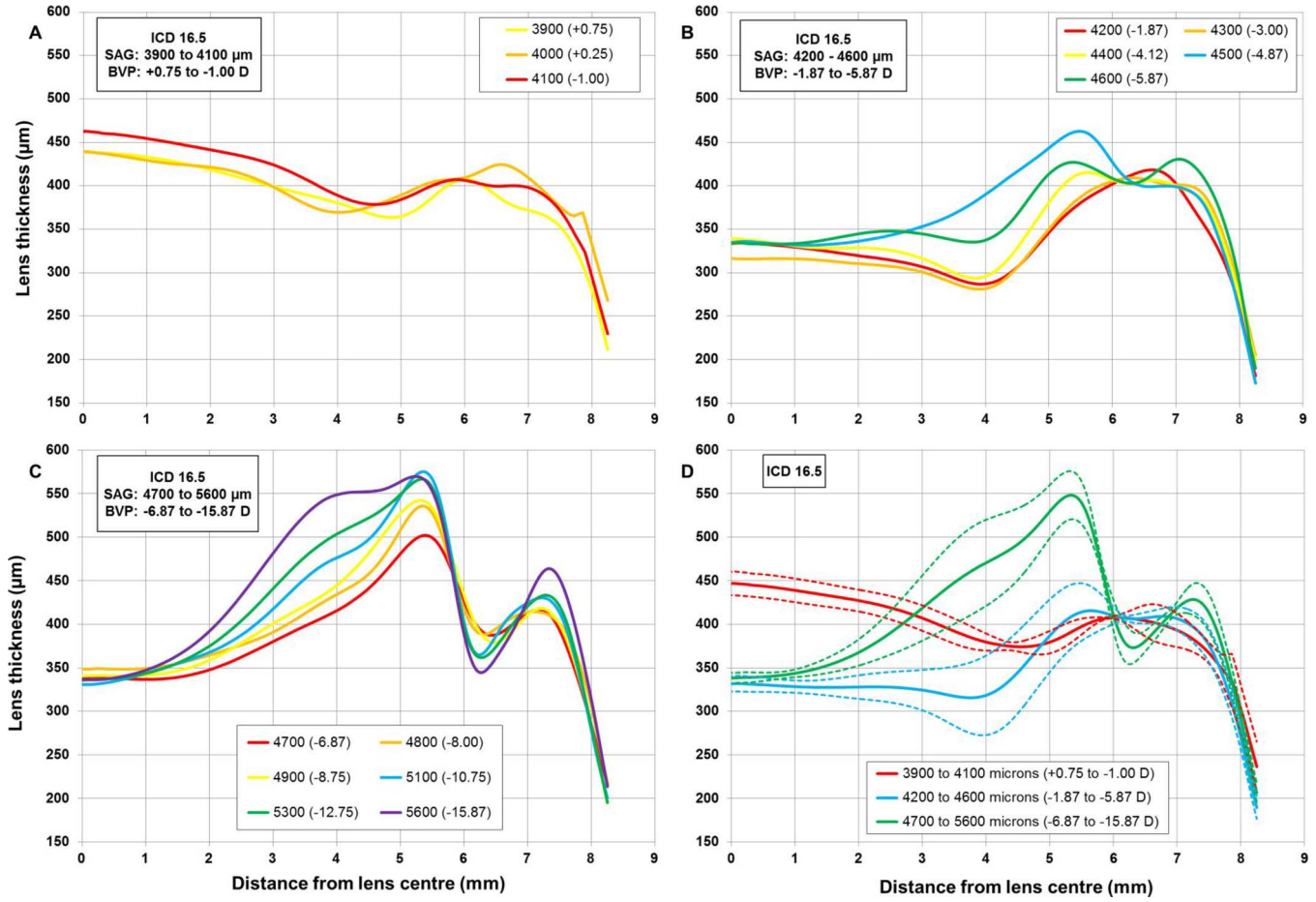

Fig. 6. Individual lens thickness profiles across a half-diameter (from lens centre to edge) for the ICD 16.5 lens design for a range of trial lenses with low (3900 to 4100 µm) (A), moderate (4200 to 4600 µm) (B), and deep sagittal heights (4700 to 5600 µm) (C). Mean lens thickness profiles for each sagittal height group in (A), (B) and (C) are displayed in (D). The solid lines in (D) represent the mean and the dashed lines represent one standard deviation of the mean.

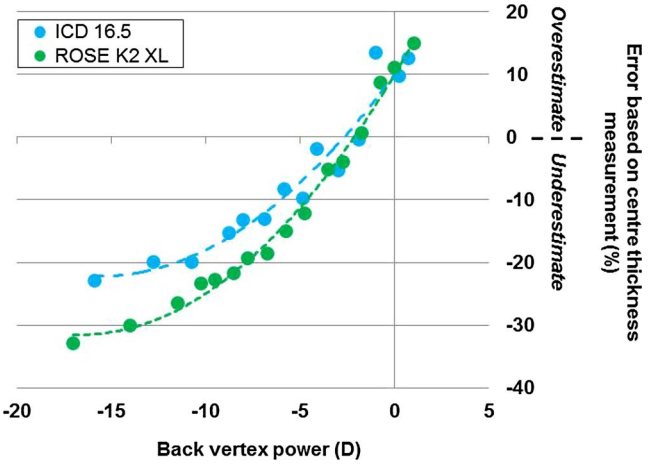

Fig. 7. Percentage error (over or underestimation of the average lens thickness) based on centre thickness measurements as a function of back vertex power for the ICD 16.5 (blue) and Rose K2 XL (green) miniscleral lenses. (For interpretation of the references to colour in this figure legend, the reader is referred to the web version of this article.)

thickness profile across the entire lens (up to 16.5 mm total diameter). This technique was highly repeatable for measures of average lens thickness compared between two orthogonal meridians of the same lens (mean relative difference 1 ± 3 µm) and displayed a high level of agreement with a manual lens gauge (estimated to the nearest micron) for measures of centre lens thickness (mean relative difference 5 ± 9 µm). While a manual lens gauge or radiuscope can be used in clinical practice to determine the lens thickness at a single location (e.g. the centre or edge thickness), this OCT imaging technique was developed in order to examine the thickness profile across the entire lens and investigate the relationship between centre and average thickness values and the variation in the difference between the average and centre thickness values with increasing back vertex powers.

As expected, based on previous studies of soft contact lenses [10,11] and the peripheral edge thickness of corneal rigid lenses [24], lens thickness varied significantly with distance from the lens centre for all scleral designs (Figs. 4–6), with the difference between the minimum and maximum thickness reaching 200–400 µm for high minus lenses (Tables 2 and 3). In general, low plus and minus powers (± 1.00 D) for the Rose K2 XL and ICD 16.5 minisclerals were thicker centrally and thinned towards the lens edge, with a secondary peak in lens thickness outside the optic zone approximately at the centre of the haptic zone (6–7 mm from the lens centre). Moderate minus powers (up to −11.25 D for the Rose K2 XL and −5.87 D for the ICD 16.5) were thinner centrally, increased in thickness to the edge of the optic zone and then gradually thinned to the lens edge, while higher minus powers displayed an additional peak in thickness within the haptic zone (Figs. 5D and 6D). These variations in thickness from the optic zone to the lens edge will not only be influenced by the back vertex power of the lens but the type of transition between the peripheral curves (e.g.

blended or sharp). These findings are in general agreement with the variations in lens thickness for smaller diameter soft contact lenses over a range of back vertex powers [1,2,10] and have implications for accurately estimating the oxygen transmissibility of scleral contact lenses.

A significant finding from our study was that the centre lens thickness in isolation significantly over or underestimated the average lens thickness for a wide range of back vertex powers (Fig. 7), a trend that was observed for two different miniscleral designs (the Rose K2 XL and the ICD 16.5) consistent with previous soft lens modelling [1,2]. For back vertex powers of −5.00 D or greater, the centre thickness underestimated the average lens thickness by between 10 and 33%, illustrating that the increased lens thickness towards the edge of the optic zone (in minus powers) and within the haptic zone, makes a substantial contribution to the average lens thickness. Reanalysis of the thickness data in Fig. 7 restricted to a central 12 mm diameter (i.e. the central region approximately covering the cornea with no lens decentration), revealed almost the same relationship, indicating that thickness variations due to the back vertex power are the primary source of over or underestimation (i.e. changes largely within the peripheral optic zone or the transition to the haptic) rather than the thickness profile of the scleral landing zone. This is an important consideration for modelling the oxygen transmissibility of scleral contact lenses and indicates that an average lens thickness, derived from the entire lens or the central 12 mm, will be a more appropriate parameter than central lens thickness for miniscleral lens designs. For example, the Dk/t of an ICD 16.5 (6.49 mm/−8.00 D, hexafocon A material) miniscleral lens based on the central thickness measurement would be 29 (cm/s)/(mlO_2/ml × mmHg), compared to 25 (cm/s)/(mlO_2/ml x mmHg) based on the average lens thickness (i.e. a 13% overestimation in lens oxygen transmissibility). Similarly, for a Rose K2 XL (6.8 mm/−7.75 D, tisilfocon A material) the Dk/t based on the central lens thickness would be 88 (cm/s)/(mlO_2/ml × mmHg) compared to 71 (cm/s)/(mlO_2/ml x mmHg) using the average lens thickness (a 19% overestimation in lens oxygen transmissibility). However, it should be noted that the thickness of the post-lens tear layer and the level of tear exchange will also influence the oxygen transmissibility of a scleral lens system, in addition to the lens thickness and material permeability.

Fatt and Ruben [25] suggested that for corneal RGP's with an 8 mm optic zone diameter, the centre lens thickness was a reasonable estimate for Dk/t calculations for back vertex powers between ± 3 D as the over or underestimation relative to the average lens thickness was only 10–25%, compared to 59–122% underestimation for −9 D lenses and 41–57% overestimation for +9 D lenses. While the magnitude of over and underestimation was substantially less in our study of scleral lenses (between 10 and 33% underestimation for a wider range of minus powers) it should be noted that the miniscleral lens designs examined will have reduced tear exchange (tear exchange occurs with blinking for the Rose K2 XL while the ICD 16.5 is a sealed system) in comparison to corneal RGP's, and therefore the average thickness value may be more appropriate for all back vertex powers of scleral lenses when calculating oxygen transmissibility.

The slight overestimation of the average lens thickness based on the centre lens thickness for low plus and minus powers may explain some of the previously reported inconsistencies between theoretical modelling of oxygen transmission and short-term clinical studies of the corneal response to scleral contact lenses. These studies have examined the corneal response following miniscleral lens wear in normal corneae [5,6], typically fitted with lenses of lower sagittal depths and back vertex powers, which may partially explain the lower than anticipated magnitude of corneal oedema compared to theoretical models [26].

A limitation of the current study is that the majority of our analyses were restricted to two rotationally symmetric miniscleral lens designs of similar total diameter (14.6 and 16.5 mm) with a wide range of minus powers, but only a single data point for positive powers (+0.75 D or +1.00 D). While lens thickness profiles may vary for larger diameter scleral lenses, the extent of over or underestimation of the average lens thickness based on the measurement of centre lens thickness for minisclerals with a diameter similar to those examined in this study can most likely be determined using the polynomial equations derived from Fig. 7. However, thickness profiles may vary significantly for front surface toric lenses, designs incorporating toric haptics or quadrant specific alterations, or customised lenses with an altered junctional thickness.

In conclusion, the thickness of scleral contact lenses varies substantially dependent upon the distance from the lens centre, and the average lens thickness typically increases with increasing back vertex powers. This has significant implications for modelling the oxygen transmissibility of scleral contact lens systems (i.e. the scleral contact lens and post-lens tear layer in combination) as centre lens thickness measurements underestimate the average lens thickness by up to 33% for high minus powers. An average lens thickness value derived from data sampled across the entire lens (or along a half-diameter for rotationally symmetric designs), or the central 12 mm covering the cornea, provides a more accurate representation of the true lens thickness and this average thickness value should be used to determine miniscleral contact lens Dk/t values.

References

[1] N.A. Brennan, Average thickness of a hydrogel lens for gas transmissibility calculations, Am J Optom Physiol Opt 61 (1984) 627–635.
[2] I. Fatt, The definition of thickness for a lens, Am J Optom Physiol Opt 56 (1979) 324–337.
[3] E.-S. Visser, R. Visser, H.J.J. Van Lier, H.M. Otten, Modern scleral lenses Part I: clinical features, Eye Contact Lens 33 (2007) 13–20.
[4] K.W. Pullum, A.J. Hobley, C. Davison, 100+ Dk: does thickness make much difference? J Br Cont Lens Assoc 14 (1991) 17–19.
[5] S.J. Vincent, D. Alonso-Caneiro, M.J. Collins, Corneal changes following short-term miniscleral contact lens wear, Cont. Lens Anterior Eye 37 (2014) 461–468.
[6] S.J. Vincent, D. Alonso-Caneiro, M.J. Collins, A. Beanland, L. Lam, C.C. Lim, et al., Hypoxic corneal changes following eight hours of scleral contact lens wear, Optom Vis Sci 93 (2016) 293–299.
[7] C. Arlt, Clinical effect of tear layer thickness on corneal edema during scleral lens wear, Aalen University, Germany, 2015 M.Sc Thesis.
[8] F. Esen, E. Toker, Influence of apical clearance on mini-scleral lens settling, clinical performance, and corneal thickness changes, Eye Contact Lens 43 (2017) 230–235.
[9] E. Lafosse, D.M. Romín, J.J. Esteve-Taboada, J.S. Wolffsohn, C. Talens-Estarelles, S. García-Lázaro, Comparison of the influence of corneo-scleral and scleral lenses on ocular surface and tear film metrics in a presbyopic population, Cont Lens Anterior Eye 41 (2018) 122–127.
[10] A. Bruce, Local oxygen transmissibility of disposable contact lenses, Cont Lens Anterior Eye 26 (2003) 189–196.
[11] J.H. Ko, A method to measure oxygen permeability of contact lenses with non-uniform thickness, Int Cont Lens Clin (1980) 36–40.
[12] V. Westphal, A. Rollins, S. Radhakrishnan, J. Izatt, Correction of geometric and refractive image distortions in optical coherence tomography applying Fermat's principle, Opt Express 10 (2004) 397–404.
[13] A. Podoleanu, I. Charalambous, L. Plesea, A. Dogariu, R. Rosen, Correction of distortions in optical coherence tomography imaging of the eye, Phys Med Biol 49 (2004) 1277–1294.
[14] K. Karnowski, I. Grulkowski, N. Mohan, I. Cox, M. Wojtkowski, Quantitative optical inspection of contact lenses immersed in wet cell using swept source OCT, Opt Lett 39 (2014) 4727–4730.
[15] M. Romero-Jiménez, P. Flores-Rodríguez, Utility of a semi-scleral contact lens design in the management of the irregular cornea, Cont. Lens Anterior Eye 36 (2013) 146–150.
[16] C. Suarez, V. Madariaga, B. Lepage, M. Malecaze, P. Fournié, V. Soler, et al., First experience with the ICD 16.5 mini-scleral lens for optic and therapeutic purposes, Eye Contact Lens 44 (2018) 44–49.
[17] M.J.A. Girard, N.G. Strouthidis, C.R. Ethier, J.M. Mari, Shadow removal and contrast enhancement in optical coherence tomography images of the human optic nerve head, Invest Opthalmol. Vis Sci 52 (2011) 7738–7748.
[18] J. Tian, P. Marziliano, M. Baskaran, H.T. Wong, T. Aung, Automatic anterior chamber angle assessment for HD-OCT images, IEEE Trans Biomed Eng 58 (2011) 3242–3249.
[19] S.A. Read, D. Alonso-Caneiro, S.J. Vincent, A. Bremner, A. Fothergill, B. Ismail, et al., Anterior eye tissue morphology: scleral and conjunctival thickness in children

and young adults, Sci Rep 6 (2016) 33796.
[20] D. Alonso-Caneiro, S.A. Read, S.J. Vincent, M.J. Collins, M. Wojtkowski, Tissue thickness calculation in ocular optical coherence tomography, Biomed Opt Express 7 (2016) 629–645.
[21] A.J. Yezzi, J.L. Prince, An Eulerian PDE approach for computing tissue thickness, IEEE Trans Med Imaging 22 (2003) 1332–1339.
[22] BSI Standards Publication, Ophthalmic optics – contact lenses. Part 2: Tolerances (ISO 18369-2:2017), 2017.
[23] J. Bland, D. Altman, Measuring agreement in method comparison studies, Stat Methods Med Res 8 (1999) 135–160.
[24] M. Guillon, J. Crosbie-Walsh, D. Brynes, Application of pachometry to the measurement of rigid contact lens edge profile, J Brit Cont Lens Assoc 10 (1987) 16–22.
[25] I. Fatt, C.M. Rubent, A simple formula for calculating the harmonic average oxygen transmissibility of an optically powered RGP contact lens, J Br Cont Lens Assoc 17 (1994) 115–118.
[26] L. Michaud, E. van der Worp, D. Brazeau, R. Warde, C.J. Giasson, Predicting estimates of oxygen transmissibility for scleral lenses, Cont Lens Anterior Eye 35 (2012) 266–271.